https://doi.org/10.5194/egusphere-2026-4456
Preprint. Discussion started: 5 August 2026

Sedimentary carbon stocks and microbial turnover in shallow coastal areas of the Baltic Sea

Nishant Nishant[1], Janina Pykäri[2], Roel Lammerant[2], Anna Villnäs[2], Camilla Gustafsson[2], Alf Norkko[2], Gregory Cowie[3], Tom Jilbert[1]

[1]Department of Geosciences and Geography, Faculty of Science, University of Helsinki, Gustaf Hällströmin katu 2, Helsinki, 00560, Finland

[2]Tvärminne Zoological Station, Faculty of Biological and Environmental Sciences, University of Helsinki, J. A. Palménin tie 260, Hanko, 10900, Finland

[3]Marine Geosciences Group, School of Geosciences, Edinburgh University, James Hutton Road, Edinburgh, EH9 3FE, United Kingdom

Correspondence to: Nishant Nishant (nishant.nishant@helsinki.fi)

Abstract. Coastal sediments play a significant role in active global carbon cycling, and their potential is well recognised for carbon sequestration. The role of shallow nearshore sediments as carbon reservoirs remains poorly constrained, particularly in heterogeneous depositional environments with varying hydrodynamic forcing, sediment texture, and organic-matter composition. Such spatial variability may decouple sediment carbon stocks from remineralisation rates, requiring carbon storage to be evaluated together with active remineralisation. To address spatial patterns in sedimentary organic carbon (C_{org}) stock and turnover potential, we sampled 20 sites at 3–4 m water depth along a strong gradient of salinity and wave exposure in the coastal zone of Hanko peninsula, Finland. At each site, two cores were collected for sediment and porewater to quantify particulate and dissolved carbon and nitrogen. Sedimentary C_{org} stocks in the uppermost 25 cm ranged from 77 to 3903 g C m^{-2}. The maximum value for fractional turnover of the stock in the uppermost 10 cm, estimated from diffusive fluxes of dissolved inorganic carbon and ammonium, was ~14% yr^{-1}. C_{org} stocks decreased with increasing depth-attenuated wave exposure, consistent with hydrodynamic sorting and reduced fine-sediment retention in exposed areas. We found that the highest proportional turnover occurred in carbon-rich sediments, implying that large C_{org} stocks are also zones of more active remineralisation. Furthermore, we explored whether bulk organic-matter source indicators, including C/N and $\delta^{13}C$, are related to fractional turnover estimates. This exercise indicated that bulk organic-matter source indicators covaried with depositional setting rather than directly controlling carbon reactivity. Our findings highlight the importance of sheltered nearshore sediments for carbon storage while showing that depositional carbon-rich areas can remain active zones of microbial remineralisation. Spatial assessments of shallow coastal carbon storage should therefore consider C_{org} stocks together with dynamic remineralisation to better constrain their carbon retention and sequestration potential.

1 Introduction

Marine sediments represent major long-term carbon reservoirs, linking organic matter (OM) deposition, processing and burial over ecological to geological timescales (Atwood et al., 2020; Burdige, 2007; Hedges and Keil, 1995). The potential of sediments to act as natural carbon sinks is thus important for climate change mitigation. Coastal areas are highly active biogeochemical zones where terrestrial inputs, marine production and lateral transport create heterogeneity in sedimentary environments along the coastal continuum that may influence carbon accumulation (Bauer et al., 2013; Veselić et al., 2025). The classical framework for *blue carbon* research has mainly focused on accumulation of carbon in vegetated coastal habitats such as seagrass, salt marshes and

https://doi.org/10.5194/egusphere-2026-4456
Preprint. Discussion started: 5 August 2026

mangroves (Duarte et al., 2005; Macreadie et al., 2019; McLeod et al., 2011). However, recent research has shown that near-shore coastal sediment carbon storage is not controlled by vegetation alone, but rather a combination of sediment texture, hydrodynamic exposure, geomorphology, and local depositional conditions as highlighted by habitat-specific studies (Röhr et al., 2018; Wikström et al., 2025).

A major challenge in assessing large scale coastal carbon storage is the strong spatial variability of sediment carbon stocks. Such variability complicates the upscaling of site-level measurements to coastal seascapes and regional carbon inventories. Site-specific stocks in the uppermost 25cm of the sediment column can vary from a few hundred to more than 26,000 g C m^{-2}, reflecting differences in sediment composition, organic matter input, burial conditions, and post-depositional degradation (Röhr et al., 2018). Recent work from the northern Baltic Sea suggests that shallow semi-enclosed bays may act as "non-classical" blue-carbon reservoirs, where coastal morphology and hydrodynamic sheltering promote the deposition and accumulation of fine-grained, organic-rich sediments (Gubri et al., 2025; Wikström et al., 2025).

Assessing the reactivity of OM is crucial for understanding the potential for long-term preservation (Smeaton and Austin, 2022). Reactivity can be investigated by molecular and compositional indicators, thermal-stability approaches such as thermogravimetric analysis or ramped pyrolysis/oxidation, and process-based estimates of reaction products produced during organic-matter degradation (Arndt et al., 2013; Chen et al., 2024; Hemingway et al., 2017). Alternatively, porewater solute profiles and diffusive fluxes may be used to estimate in situ OM degradation rates. This approach utilizes measurements of dissolved inorganic carbon (DIC) and nutrients that accumulate in porewaters and may be transported across the sediment–water interface (Berner, 1980; Burdige, 2007). Porewater concentration gradients and diagenetic models therefore provide useful indicators of active OM processing and can complement stock-based assessments of sedimentary carbon storage.

The northern Baltic Sea is characterized by strong anthropogenic eutrophication since the mid-20th century, in which enhanced OM loading increases the rates of microbial remineralization, oxygen demand, and nutrient release from sediments (Conley et al., 2011; Jilbert et al., 2021; Kuliński et al., 2022). Moreover, modern sedimentation in this region integrates inputs of carbon from both terrestrial and marine sources, whose abundance may vary greatly along gradients from freshwater to brackish marine settings (Jilbert et al., 2018). These factors along with broad mosaic of seafloor habitats, lead to high potential for heterogeneity in carbon stocks and reactivity, which need to be determined to understand the overall role of coastal sediments in carbon storage. Although large-scale marine carbon inventories increasingly recognise spatial variability in sediment carbon stocks, robust coastal carbon-cycle assessments require linking carbon storage with porewater derived diffusive fluxes, across heterogeneous seascapes such as estuary–archipelago systems.

Here we present a study of sedimentary organic carbon (C_{org}) stocks and porewater-derived diffusive fluxes of remineralization products along an estuary-archipelago exposure gradient in near-shore environments of the northern Baltic Sea. We show how C_{org} storage and gross remineralization is related to hydrodynamic exposure and investigate factors controlling the rate of turnover of the standing carbon stock, including bulk OM source indicators.

2 Study area

https://doi.org/10.5194/egusphere-2026-4456
Preprint. Discussion started: 5 August 2026

The study area is situated in the northern Baltic Sea at the entrance to the Gulf of Finland (Fig. 1a). The Gulf of Finland has an average depth of around 37 m and maximum depth of 123 m near the connection to the Baltic Proper (Alenius et al., 1998). The northern coast of the Gulf is characterised by an irregular archipelago seascape with numerous bays, peninsulas, islands and shallow basin systems. Brackish salinities in the region reflect strong freshwater influence from riverine input diluting saline water masses from the southern Baltic Sea. Oxygen deficient zones are common in deeper or poorly ventilated basins, whereas shallow areas generally maintain oxic conditions due to wind-driven mixing and a shallow water column (Conley et al., 2011; Vallius, 2006; Virtasalo et al., 2005).

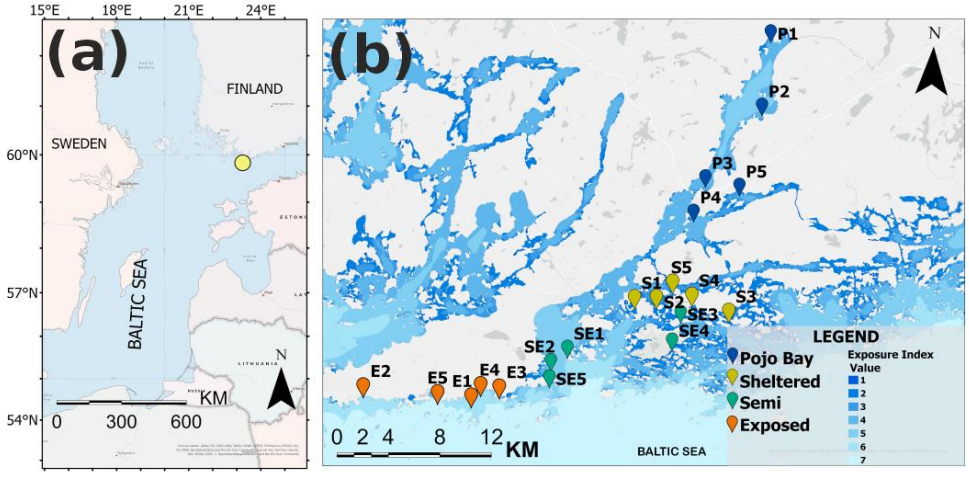

Figure 1: (a) Study area location (yellow mark) in Southern Finland. (b) Sampled sites divided into four categories representing Pojo Bay (estuary), Sheltered (inner-archipelago), Semi-Exposed (middle-archipelago) and Exposed (outer archipelago) with five sites each, along with surface wave exposure index (Surface wave exposure file/ Source: Syke, ELY Centers). Low values are indicative of low wave exposure and vice versa. Map created using ArcGIS Pro 3.4.0.

Sedimentation regime in the complex archipelago-estuary system is highly spatially heterogeneous, reflecting the interaction of glacial seafloor morphology with current hydrodynamic setting. The retreat of the Weichselian ice sheet produced an irregular seafloor with bedrock highs, eroded basins, eskers and sediment deposition areas (Winterhalter, 1992). In the modern setting, sheltered embayments and depressions generally favour the retention of fine-grained, organic-rich postglacial muds, whereas more open shallow areas are more prone to wave- and current-driven sediment resuspension, sorting, reworking, or non-deposition (Virtasalo et al., 2005; Winterhalter, 1992). Continuous glacio-isostatic uplift, which is currently occurring in the region at a rate of about 4–6 mm $year^{-1}$ (Atwood et al., 2020; Burdige, 2007; Hedges and Keil, 1995), further alters basin connectivity and coastal bathymetry, progressively altering the balance between accumulation, transport, and erosion throughout the archipelago seafloor.

Pelagic and benthic primary production in the study area varies seasonally. The phytoplankton spring bloom is commonly dominated by diatoms and dinoflagellates while summer blooms generally comprise a more diverse assemblage with a greater contribution from filamentous cyanobacteria. Although the pelagic biomass production

https://doi.org/10.5194/egusphere-2026-4456
Preprint. Discussion started: 5 August 2026

is highest during the spring bloom, the highest export of bloom-derived particulate C_{org} to the seafloor reaches its annual maximum in August (Uth et al., 2024). In autumn, macrophyte biomass and eventually C_{org} stock is at its highest (Lammerant et al., 2025). Furthermore, at these shallow coastal areas, microphytobenthic communities in illuminated seafloor can contribute significantly to autochthonous production (Virta et al., 2019). Shallow-water photic benthic habitats along the estuary-archipelago gradient consist of a heterogeneous mosaic of hard-bottom and soft-sediment habitats, which differ in substrate type, vegetation structure, biological composition and ecosystem functioning. These include hard bottom communities dominated by *Fucus vesiculosus* canopies and blue mussel beds like *Mytilus trossulus* (Attard et al., 2019; Rodil et al., 2021). The vegetated habitats along the gradient are highly heterogenous, covering a spatially structured set of aquatic plant meadows differing in species composition and carbon storage potential (Lammerant et al., 2025).

In addition, the study area receives allochthonous C_{org} as riverine and catchment-derived dissolved OM, primarily during the spring snowmelt and runoff (Asmala et al., 2016). The whole region has been eutrophied due to nutrient inputs from land-use change, fertilizer use and waste waters, in particular since 1950 (Gustafsson et al., 2012). Previous work in the study area has demonstrated a high demand for oxygen and other electron acceptors in the sediments, caused by elevated inputs of autochthonous and terrestrial OM. This has led to enhanced methanogenesis and shoaling of the sulfate-methane transition zone (Jilbert et al., 2021). Along the estuary-archipelago transect, salinity, flocculation of iron (Fe) and OM, and lateral variability in reactive sediment components have further influenced the vertical diagenetic zonation and redox-sensitive processes in sediment column (Jilbert et al., 2018). Near-shore soft-bottom sediments along the estuary-archipelago gradient typically accumulate under oxic bottom waters and therefore support macrofaunal communities involved in bioturbation and bioirrigation. Inner-archipelago sediments are frequently linked with smaller, surface-active fauna, whereas outer-archipelago sediments can support larger, deeper-burrowing taxa (Villnäs et al., 2019). Such spatial variability in macrofaunal community structure is relevant to sediment mixing, oxygen penetration, redox zonation, OM turnover and nutrient cycling (Carstensen et al., 2014; Villnäs et al., 2012).

3 Field sampling and methods

The study area spans an estuary-archipelago gradient of approximately 50 km, including the coastal region of Hanko Peninsula, Tvärminne Archipelago, and Pojo Bay located in Southern Finland (Fig. 1b). Throughout the study area, salinity and wave exposure increase towards the outermost sampling locations. Based on geographical location and prior knowledge of vegetated areas, the study was divided into four categories: Pojo Bay (estuary), Sheltered (inner archipelago), Semi-exposed (middle archipelago) and Exposed (outer archipelago) with each category containing 5 sites (Fig. 1b). The twenty sites were sampled during a field campaign in August - September 2023. Sampling for sediments, vegetation and fauna was performed by SCUBA diving at two water depths: shallow (1–2 m) and deep (3–4 m). For this study, sediment hand cores (0 – max. 30 cm sediment depth) were collected at the second water depth only (3–4 m water depth) for sediment solid phase analyses and porewater chemistry. Salinity, dissolved oxygen and temperature were measured using YSI ProSolo ODO/CT at 1 m water depth at each sampled site and depth. The sediment coring locations were close to vegetated areas but in most cases, vegetation was not present at the 3–4 m depth zone where the cores were taken.

3.1 Solid phase analyses

https://doi.org/10.5194/egusphere-2026-4456
Preprint. Discussion started: 5 August 2026

Sediments from the hand cores were sliced at 2 cm intervals (0–30 cm or base of core if <40 cm) into plastic bags and stored frozen at -20°C. Water content was estimated from mass loss during freeze drying (24 to 72h, based on type of sediments). Organic matter content (OM%) was determined on subsamples from each depth interval using TGA701 Thermogravimetric analyzer (TGA) as Loss on Ignition (LOI) at 550 °C. After OM removal, grain size distribution of the residual sediment was determined by particle size analyser (Microtrac SYNC 3R/Img L). Parallel subsamples from every second depth interval were analysed by Leco CN828 analyser for total carbon (C_{tot}) and nitrogen (N_{tot}) content. Subsamples from intervening depths were analysed by stable isotope mass spectrometer (CF-SIRMS) coupled with a FlashEA1112 elemental analyzer for $\delta^{13}C$ and $\delta^{15}N$, and total carbon (C_{tot}) and nitrogen (N_{tot}) respectively. The $\delta^{13}C$ and $\delta^{15}N$ values are reported relative to Vienna Pee Dee belemnite (VPDB). C_{tot} is considered equal to organic carbon (C_{org}). Tests with TGA at 900°C and Leco CN828 analysis of samples after LOI at 550°C showed that the contribution of inorganic carbon to C_{tot} in this region is likely <5%, concurring with recent estimates (Wikström et al., 2025).

3.2 Porewater sampling and treatment

The hand cores were pre-drilled with two vertical columns of holes labelled *A* and *B* (5 mm diameter, 2 cm interval) and taped prior to the sampling. Porewater samples were collected using Rhizons™ inserted through the holes (membrane pore size 0.15 µm) into syringes (10 ml) held at vacuum, immediately after the core recovery. The syringes for column *A* were pre-loaded with 1 ml of 0.1 M HNO_3 to convert all dissolved inorganic carbon (DIC) to CO_2 (Jilbert et al., 2020) while the syringes for column *B* were empty. After collection of at least 3 ml of sample, syringes were placed in coolbox until further processing.

In the laboratory, column *A* samples were processed as follows: Acquired sample volumes in the syringes were noted, and a known volume of N_2 gas (quality 5.0) was injected to create a headspace. Syringes were then shaken for 5 minutes to equilibrate gaseous substances between the headspace and dissolved phase. After equilibration, 5 ml headspace gas was transferred via a dry syringe to pre-evacuated Labco Exetainers (12 ml). An additional 7 ml of N_2 gas (quality 5.0) was added to equalize pressure. From column *B*, 2 ml subsamples were taken for trace elemental analysis into a centrifuge tube preloaded with 10 µL of 65% HNO_3. The remaining sample was stored frozen at -20°C prior to analysis of dissolved ammonium (NH_4^+).

3.3 Porewater analyses

Total dissolved iron (Fe^{2+}) and total dissolved sulphur (assumed primarily as SO_4^{2-} due to loss of H_2S during acidification) in porewater were analyzed by Agilent 8900 ICP-MS (QQQ). Analysis of ammonium (NH_4^+) was performed using a Hitachi U-1100 Shimadzu spectrophotometer. For DIC and CH_4, the Exetainers with gas samples were pressurized with pure Helium before injecting the sample into a Gas Chromatograph (GC) (Agilent Technologies 7890B) equipped with a thermal conductivity detector (TCD) and flame ionization detector (FID) to measure CO_2 (DIC) and dissolved methane (CH_4) respectively against standard mixtures as described by Jilbert et al. (2020).

4 Calculations

4.1 Carbon stocks

https://doi.org/10.5194/egusphere-2026-4456
Preprint. Discussion started: 5 August 2026

Solid phase density of bulk sediment was estimated according to Eq. (1). Including the lower density of OM relative to minerogenic matter in the equation reduces the uncertainty identified by Chatting et al. (2025) concerning estimates of dry bulk density (DBD) derived from assumed solid phase densities rather than direct volumetric measurements.

Porosity was determined from solid phase density and gravimetric water content according to equations in the supplement of Lindroth-Dauner et al. (2026). Wet bulk density (WBD) and dry bulk density (DBD) were then estimated according to Eqs. (2) and (3). Sedimentary C_{org} stocks reported as g C m^{-2} for a given thickness of the sediment column were estimated according to Eq. (4) from DBD, C_{org} content and the volume of sediment, as a sum of the values for the 2 cm slices of the sediment cores.

$$\text{Solid phase density } \left(\frac{g}{cm^3}\right) = 1.4 \times \left(\frac{OM}{100}\right) + 2.65 \times \left(1 - \frac{OM}{100}\right) \quad (1)$$

where 1.4 g/cm^3 is the density of pure OM and 2.65 g/cm^3 is the density of mineral phases (Burdige, 2006; Pajunen, 2000).

$$\text{WBD } \left(\frac{g}{cm^3}\right) = [(\Phi \times 1) + (1 - \Phi) \times \text{Solid phase density})] \quad (2)$$

$$\text{DBD } \left(\frac{g}{cm^3}\right) = \frac{\text{Sediment content (\%)}}{100} \times WBD \quad (3)$$

$$C_{org}\ stock\ \left(\frac{g}{m^2}\right) = \Sigma_{length\ of\ core}^{top} \left(\left(\frac{C_{org}\ (\%)}{100}\right) \times DBD\left(\frac{g}{cm^3}\right) \times Volume(cm^3)\right) \quad (4)$$

where Φ is volumetric porosity and sediment content (% relative to sample weight) is calculated from wet and dry weight of samples. Volume (cm^3) = volume of sediment in each 2-cm-thick slice of the 1 m^2 column (i.e. 20000 cm^3). The length of sediment cores recovered was variable (Table 1). To align with other studies, we extrapolated the C_{org} stock to the top 25 cm using a linear regression of depth with the stock in the lowermost 6 cm portion of the measured interval.

Table 1: Physicochemical parameters (1 m water depth) and depth-attenuated wave-exposure (SWM(d)) at 3.5 m water depth along with the Mean ± standard deviation (SD) of loss-on-ignition (LOI), organic carbon (C_{org}), dry bulk density (DBD), median grain size (D50 µm), mud (clay+silt) content (<63 µm), C/N ratio (mol) and isotope $\delta^{13}C$ of the respective sites. The sediment core sliced with 2cm depth interval. Pojo Bay

Category	Site	Water depth (m)	Core depth (cm)	In situ T (°C)	Salinity (PSU)	Oxygen (mg L^{-1})	SWM(d)	DBD±SD (g cm^{-3})	LOI±SD (%)	C_{org} ±SD (%)	D50±SD (µm)	Mud ±SD (%)	C/N ± SD (mol)	$\delta^{13}C$ ± SD (‰)
Pojo Bay	P1	3.5	22	18.2	1.59	8.97	0.2	0.4 ± 0.0	6.16 ± 0.25	2.05±0.18	40.9 ± 5.8	78.3±10.3	10.18±0.44	-26.43±0.67
	P2	3.2	22	17.9	1.53	10.28	19.5	0.3 ± 0.1	12.77 ± 3.23	3.89±0.82	33.3 ± 8.4	85.8 ±7.6	9.56±0.60	-23.92±1.58
	P3	3.7	22	18.1	1.85	10.05	0.0	0.6 ± 0.0	4.89 ± 0.76	1.51±0.21	38.7 ± 5.0	81.5 ±7.7	9.64±0.30	-24.06±0.04
	P4	3.2	30	17.4	3.29	9.60	6.5	0.4 ± 0.1	8.12 ± 1.96	2.84±0.74	36.0 ± 3.8	86.6 ±5.0	9.80±0.26	-23.58±1.21
	P5	1.7	20	17.6	3.01	8.91	813.3	0.4 ± 0.1	8.66 ± 1.26	3.26±0.58	38.5 ± 1.8	82.6 ±2.6	9.88±0.48	-25.03±0.94
	S1	3.7	24	19.6	5.82	9.61	3476.7	1.6 ± 0.4	1.90 ± 1.38	0.46±0.36	49.5 ± 31.9	62.5 ±27.7	7.99±2.39	-24.24±1.15

https://doi.org/10.5194/egusphere-2026-4456
Preprint. Discussion started: 5 August 2026

Sheltered	S2	4	20	20.1	5.42	10.47	1849.2	1.4 ± 0.1	0.82 ± 0.25	0.16±0.12	32.5 ± 27.9	80.1 ±24.3	8.74±3.52	-24.94±1.17
	S3	3.9	22	18.1	6.13	8.66	699.5	0.4 ± 0.1	10.57 ± 3.01	3.59±0.97	37.0 ± 7.9	81.5 ±12.1	9.04±0.36	-22.27±0.11
	S4	3.8	18	18.5	5.79	8.21	109.6	0.4 ± 0.0	10.35 ± 1.18	3.38±0.53	43.8 ± 3.4	74.7 ±5.8	9.04±0.25	-22.01±0.26
	S5	3.6	24	19	5.24	8.99	25.6	0.3 ± 0.0	13.92 ± 3.33	4.77±1.29	37.7 ± 7.6	81.8 ±10.1	9.11±0.82	-22.34±0.12
Semi-exposed	SE1	3.5	14	19.1	6.14	11.05	1011.0	1.5 ± 0.2	1.89 ± 0.79	0.87±0.33	100.5 ± 19.4	22.1 ±15.3	10.10±1.01	-21.89±0.94
	SE2	3.6	20	19	5.92	10.00	199.3	1.6 ± 0.1	0.76 ± 0.26	0.21±0.05	96.1 ± 22.8	11.6 ±8.2	8.16±1.10	-21.89±0.40
	SE3	4	20	18.7	5.95	9.13	6462.9	1.6 ± 0.1	0.69 ± 0.20	0.27±0.10	122.7 ± 41.2	28.3 ±8.3	7.86±1.37	-23.47±0.80
	SE4	3.3	16	18.2	6.01	8.00	3317.5	1.6 ± 0.1	1.10 ± 0.44	0.38±0.14	228.6 ± 19.6	7.7 ±6.3	8.06±1.25	-22.19±0.53
	SE5	3.2	20	17.8	6.17	9.03	4168.8	1.6 ± 0.1	0.38 ± 0.25	0.20±0.11	287.2 ± 15.0	2.1 ±4.2	6.60±2.11	-21.82±0.31
Exposed	E1	3.3	18	18	6.42	10.09	17554.1	1.6 ± 0.1	0.78 ± 0.26	0.17±0.07	150.5 ± 6.6	1.6 ±0.5	7.04±1.46	-20.77±0.77
	E2	4.6	12	18.1	6.31	9.59	6545.0	2.0 ± 0.2	1.09 ± 0.48	0.20±0.07	142.7 ± 15.1	4.8 ±3.6	5.34±0.93	NA
	E3	3.5	20	18.6	6.43	9.42	19351.7	1.7 ± 0.1	0.80 ± 0.54	0.14±0.08	364.7 ± 121.0	1.3 ±3.7	6.28±2.45	-21.80±0.44
	E4	3.7	14	18.3	6.29	9.17	12651.1	1.6 ± 0.1	2.05 ± 1.21	0.17±0.02	390.8 ± 57.6	0.1 ±0.1	5.09±0.42	NA
	E5	3.1	20	18.1	6.39	9.21	27930.2	1.7 ± 0.0	0.04 ± 0.05	0.01±0.01	286.7 ± 24.1	0.0 ±0.0	0.27±0.38	NA

4.2 Dissolved inorganic carbon and methane

Methane and DIC concentrations were estimated from GC measurements as follows. Peak areas in the headspace samples were converted to ppm (mole fraction) by linear calibration with standards. Measurements of CO_2 and CH_4 in the standard within the series were used to monitor drift and adjusted accordingly.

The ideal gas law and Henry's law (Eq. 5) were then utilised to back-calculate the in situ dissolved gas concentration ($Conc_{tot}$, mol L^{-1}) from measured concentration (ppm) in the headspace gas.

$$Conc_{tot} = \frac{\frac{P_{hs} \times V_{hs}}{R \times T} + F \times P_{hs} \times V_{aq}}{V_{aq}} \quad (5)$$

where P_{hs} is the partial pressure of the gas in headspace (atm), V_{hs} is headspace volume (L), V_{aq} is the water volume (L), R is the gas constant, T is the equilibrium temperature (Kelvin) and F is the temperature and salinity dependent equilibrium coefficient described by Weiss and Price (1980) for CO_2 and Wiesenburg and Guinasso (1979) for CH_4. Estimation of $Conc_{tot}$ was further simplified assuming total pressure (P_{atm}) during equilibrium in the syringe is 1 atm and P_{hs} was expressed as $P_{atm} \times X_{hs}$, where X_{hs} is the mole fraction of gas measured (ppm) from the headspace.

The samples were run in two batches interspersed with blank and standard measurements. Previous studies have shown that the pre-evacuated Exetainers can be contaminated with a small amount of air (Sturm et al., 2015). Cut-off CO_2 and CH_4 concentrations were thus calculated for each batch, below which the measured concentrations were considered indistinguishable from the contamination. Errors due to diffusive loss of gas through use of plastic syringes in the sampling method has been established to be negligible (Myllykangas et al., 2017).

4.3 Approaches to estimate microbial turnover of carbon from porewater profiles

https://doi.org/10.5194/egusphere-2026-4456
Preprint. Discussion started: 5 August 2026

Three independent approaches were applied to estimate the extent of microbial mineralization of carbon from the sediment stock using porewater data. These comprise:

1. Estimate of diffusive fluxes of carbon across the sediment-water interface (SWI) using Fick's first law applied to DIC profiles: Dataset 1 (DS1) calculated using Fick's first law of diffusion (Eq. 6) based on the concentration gradient ($\frac{dC}{dx}$) between the bottom water (BW) and the uppermost porewater (f_PW) samples. Length of the diffusion pathway between these samples is set at 1 cm.
2. Estimate of diffusive fluxes of carbon across the SWI using Fick's first law applied to NH_4^+ profiles: Dataset 2 (DS2) uses the NH_4^+ concentration gradient at the SWI using Eq. (6) for BW and uppermost PW samples (in most cases the f_PW sample only, but for Semi-exposed sites the best-fit through the upper two). The calculated NH_4^+ fluxes were converted to theoretical values for DIC fluxes using sediment stoichiometry with assumption that organic matter degradation releases C and N proportional to bulk sediment C/N composition (Table 1). Length of the diffusion pathway between BW and uppermost PW sample is set at 1 cm.
3. Estimate of rate of production of dissolved carbon in the sediment column using Fick's second law applied to NH_4^+ profiles: Dataset 3 (DS3) utilises all the measured porewater NH_4^+ concentration data employing the PROFILE software, which solves a 1-D mass conservation equation (Eq.7) to estimate vertical transport molecular diffusion rates by using a two-step statistical procedure. The model provided by Berg et al. (1998)performs statistical F-tests and calculates p-values to compare and identify the lowest number of zones required to explain the data without over-interpreting. A depth-integrated rate of net production or consumption of NH_4^+ was then calculated. These rates were converted to production or consumption of DIC using stoichiometry of bulk sediment C/N ratios.

Diffusive fluxes and production rates were calculated using Fick's laws of diffusion and PROFILE software as described above for DS1, DS2 and DS3. The following equations were used:

$$J = -\varphi Ds\left(\frac{dC}{dx}\right) \quad (6)$$

$$\frac{d}{dx}(-\varphi D_s \frac{dC}{dx}) + R = 0 \quad (7)$$

Ds is the bulk sediment diffusion coefficient, φ is the porosity, $\frac{dC}{dx}$ is the gradient of the concentration over depth (cm) and R is the net production or consumption rates.

Further, Ds was estimated using the equation:

$$D_s = \frac{D_0}{\theta^2} \quad (8)$$

$$\theta^2 = 1 - \ln(\varphi^2) \quad (9)$$

where D_0 is the free solution diffusion coefficient for NH_4^+ and DIC (consisting of pH specific-components of CO_2, HCO_3^-. and CO_3^{2-}), corrected for temperature and salinity, and θ is the tortuosity (Boudreau, 1997).

https://doi.org/10.5194/egusphere-2026-4456
Preprint. Discussion started: 5 August 2026

The simplified mass conservation equations assume steady state conditions and do not account for porewater advection, bio-diffusion or bio-irrigation. Therefore, the diffusion-based quantifications of carbon turnover reported in this study are minimum estimates of the likely real values. Many of the study sites are characterized by infaunal communities including *Macoma balthica, Hediste diversicolor, Marenzelleria* spp, Hydrobiidae and Chironomidae (Mäkelin et al., 2024) that physically disturb the porewaters and contribute to enhanced turnover through their own respiratory processes (Kristensen, 2000; Kristensen et al., 2012). Annual fractional turnover rates were calculated using the diffusive fluxes from the three datasets (DS1, DS2 & DS3) as the ratio of fluxes to the magnitude of the sedimentary C_{org} stock in the top 10 cm.

4.4 Wave exposure index

Wave exposure index in the study area was acquired from open access data from the Finnish Environment Institute (Fig. 1b). The data file presents a spatial estimate of wave exposure from the Simplified Wave Model (SWM). The exposure index is a 25 m resolution raster and accounts for coastal geometry by calculating effective fetch directions (16 segments), adjusted for wave refraction and diffraction. These index values are thus a product of direction-specific fetch and mean wind speed.

In addition to the spatial wave exposure layer, a depth-attenuated wave exposure metric, SWM(d) was extracted for each site, for comparison with the sediment characteristics and carbon stock. SWM(d) is also derived from the Simplified Wave Model framework and accounts for the attenuation of wave energy with increasing water depth, while retaining the effects of refraction and diffraction around coastal landforms as described by Virtanen et al. (2019). SWM(d) is reported on a relative scale and was calculated using 3.5 m water depth for all the study sites.

4.5 Statistical analyses

The correlation between pairs of variables was assessed using Pearson and Spearman tests based on the normality of the distribution (assessed by the Shapiro-Wilk test). For exploratory investigation of variations across the four categories of study sites, a non-parametric Kruskal-Wallis-test was used due to non-normal distributions and/or unequal variances, followed by post hoc pairwise comparison using Dunn's test with Holm correction for significance of differences ($p<0.05$). Further, Cliff's delta (non-parametric effect size measure) was used to evaluate the magnitude of differences among categories. To avoid pseudo-replication, each site was represented by the median value of its measured parameters. This helped to draw robust conclusions about the categorical differences in the carbon and turnover processes. Statistical analysis and visualisation were performed using Python 3.11.5.

5 Results

5.1 Physico-chemical conditions of the study sites

Dissolved oxygen concentrations during sampling were high at all sites (8.00 to 11.05 mg/L, Table 1). Water column temperature ranged from 17.4 to 20.1 °C. Salinity was in the range from 1.53 in Pojo Bay site P2 to 6.43 in Exposed site E3 (all values determined at 1 m water depth). Annual normalized values of depth-attenuated wave exposure SWM(d) vary considerably between study sites, with a generally increasing trend along the gradient from Pojo Bay to Exposed sites (Table 1).

https://doi.org/10.5194/egusphere-2026-4456
Preprint. Discussion started: 5 August 2026

5.2 Intrinsic properties of the sediments

Sediment cores showed profiles of generally declining C_{org} (% d.w.) with depth below the sediment-water interface, with some exceptions (Fig. S1). The overall ranges of C_{org} (% d.w.) varied considerably between categories (Fig. 2a). Sheltered sites showed a heterogenous distribution with lowest site-specific value of 0.16 ± 0.12 (% d.w.) at S2 and highest site-specific value of 4.77 ± 1.29 (% d.w.) at S5 (Table 1). In Pojo Bay, a more homogeneous distribution was observed, ranging from 1.51 ± 0.23 (% d.w.) at P3 to 3.89 ± 0.82 (% d.w.) at P2. Exposed and Semi-exposed sites had an average C_{org} content <1 (% d.w.). Post-hoc tests between the site categories showed significant differences only between Pojo Bay and Exposed sites for C_{org} content. However, Cliff's delta (δ) showed separation (+1) of Pojo Bay over Exposed and Semi-exposed sites and overlap with Sheltered sites for C_{org} content (Table S1).

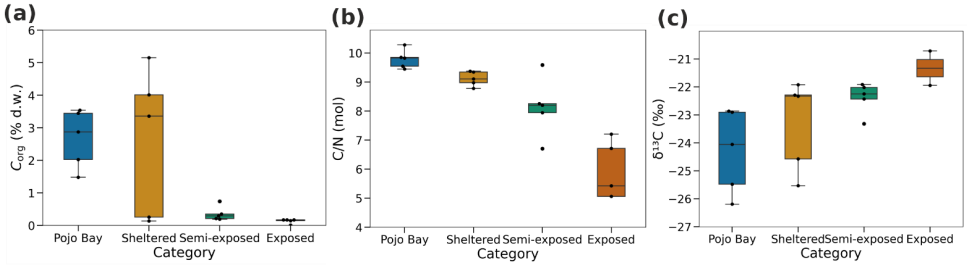

Figure 2: (a) Box and whisker plot comparing sediment median C_{org} (% d.w.), (b) C/N (mol) and (c) δ¹³C (‰) (n=5) distribution among the four categories. For δ¹³C (‰), n = 2 for the Exposed sites.

OM (% d.w.) and C_{org} (% d.w.) showed a strong linear correlation (C_{org} = 0.33OM – 0.03), with 95% of the variation in C_{org} content explained by the OM content (R^2 = 0.95, Fig. 3a). The category-specific linear regressions showed that the relationship between OM and C_{org}, however, varied along the transect. The corresponding fitted equations were: Pojo Bay: C_{org} = 0.28OM + 0.41; Sheltered: C_{org} = 0.35OM - 0.13; Semi-exposed: C_{org} = 0.38OM + 0.01; and Exposed: C_{org} = 0.06 OM + 0.08. The strongest fit was observed in Sheltered sites (R^2 = 0.96), followed by Pojo Bay (R^2 = 0.80) and Semi-exposed sites (R^2=0.74), whereas the relationship was much weaker in Exposed sites (R^2 = 0.28), where contents of both C_{org} and OM were extremely low. D50 was strongly inversely related to mud content (<63 µm; Spearman's ρ = −0.97, $p < 0.05$), confirming that it captured the dominant sand–mud gradient across the study area.

The distribution of OM% in relation to the D50 followed a distinct L-shaped pattern (Fig. 3b). Values of D50 were found to be homogeneously muddy (D50 < 6 µm) in Pojo Bay, ranging from 33.3± 8.4 µm (P2) to 40.9 ± 5.8 µm (P1), and at Sheltered sites, ranging from 32.5 ± 27.9 (S2) to 49.5±31.9 µm (S1). These categories were typically characterized by higher OM%, although the Sheltered category includes two sites of lower OM% despite the dominance of fine-grained material (Tables S1 and S2, Table 1). In contrast, sites in the Semi-exposed and Exposed categories showed higher values of D50 (96.1 ± 22.8 (SE2) to 390.8 ± 57.6 (E4)) and consistently low values of OM%. An inverse exponential decay relation was found between C_{org} and Dry bulk density (DBD), with $DBD = 1.789^{-0.516 C_{org}}$ (Fig. 3c) with 90% of variation in DBD explained by C_{org} (R^2= 0.90).

https://doi.org/10.5194/egusphere-2026-4456
Preprint. Discussion started: 5 August 2026

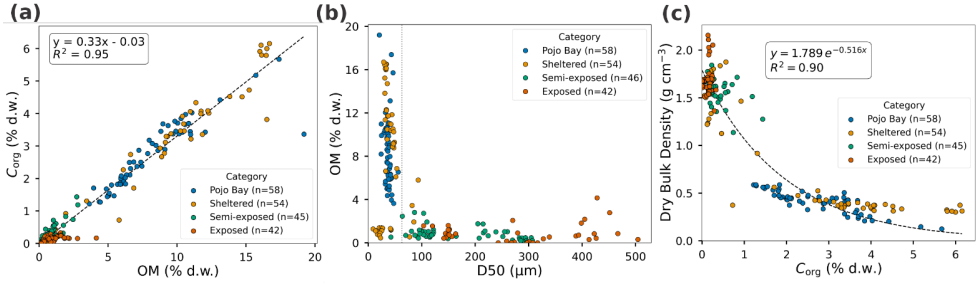

Figure 3: (a) Relation of OM % vs C_{org} (%.d.w.) and (b) median grain size (D50) vs OM %, and (c) C_{org} % vs dry bulk density of all sediment samples from all sites. No significant fit was observed between D50 and OM (% d.w.).

Along the transect, bulk sediment C/N decreased gradually (Fig. 2b) with the highest average of 10.18 ± 0.44 mol at site P1 and lowest at site E5 with 0.27±0.38 mol (Table 1). Kruskal-Wallis tests confirmed significant differences between categories, although only Pojo Bay vs. Exposed sites appeared to be significant in the post-hoc analysis (Table S1). Bulk sediment $\delta^{13}C$ showed an apparent trend towards less negative values along the transect, with site P1 having the most depleted average value of -26.43 ± 0.67 (‰) and site E1 the most enriched at -20.77±0.77 (‰). Differences in $\delta^{13}C$ among the categories were borderline significant (p = 0.05).

5.3 Carbon stock estimates and dependence on wave exposure

Carbon stocks reported for the uppermost 25 cm of the sediment column show a wide range of values (Fig. 4). The lowest site-specific stock was observed in the Exposed category (77 g C m^{-2} at site E5) and highest in the Sheltered category (3903 g C m^{-2} at site S5). On category level, highest average carbon stock sediments were found in Sheltered sites with 2347 ± 1318 g C m^{-2} followed by Pojo Bay with 2257 ± 351 g C m^{-2}, Semi-exposed with 979 ± 470 g C m^{-2} and Exposed with 506 ± 283 g C m^{-2} (Table 2). Overall, the average carbon stock across all sites was 1522 g C m^{-2} with standard deviation of 1061 g C m^{-2} which highlights the variability across the sampled study area. Regression analysis showed an exponential relationship between SWM(d) and C_{org} stock with $C_{org}stock = 1849e^{-0.0001SWM(d)}$ (R^2 = 0.51). The C_{org} stock showed a significant negative monotonic relationship with the SWM(d) (ρ =-0.75and p <0.05) indicating higher carbon stocks at sites of lower wave exposure (Table S2). Furthermore, the SWM(d) showed a significant positive monotonic correlation with D50 (ρ =0.77and p <0.05).

Table 2: Sedimentary C_{org} stock in calculated in the top 25cm and fluxes in mmol m^{-2} d^{-1} from three different approaches (DS1, DS2 & DS3) for DIC (dissolved inorganic carbon) and NH_4^+ (dissolved ammonium), along with the order of magnitude (OOM) difference for DIC. NA (Not Available).

Category	Site	Sediment carbon stock (top 25cm)	CH_4	DS1	DS2		DS3		OOM-DIC
			mmol m^{-2} d^{-1}	mmol m^{-2} d^{-1}	mmol m^{-2} d^{-1}		mmol m^{-2} d^{-1}		
		g C m^{-2}		DIC	NH_4^+	DIC	NH_4^+	DIC	
Pojo Bay	P1	1931	0.007	2.69	0.55	5.10	0.57	5.87	Same

https://doi.org/10.5194/egusphere-2026-4456
Preprint. Discussion started: 5 August 2026

	P2	2669	0.630	10.07	2.19	20.74	2.84	26.81	Same
	P3	1851	0.009	1.46	0.56	5.27	0.97	9.20	Same
	P4	2427	0.000	0.83	0.27	2.70	0.33	3.20	Same
	P5	2407	NA	NA	NA	NA	NA	NA	NA
Sheltered	S1	1781	0.000	0.08	0.50	4.80	0.55	5.20	Different
	S2	425	0.001	-1.37	0.28	2.54	0.17	1.51	Same
	S3	3006	0.000	3.68	1.35	11.41	1.72	15.39	Same
	S4	2620	0.001	8.58	1.13	9.94	1.68	15.33	Same
	S5	3903	0.002	7.47	1.56	13.65	1.75	16.03	Same
Semi-exposed	SE1	1783	0.000	1.41	0.08	0.71	0.06	0.53	Same
	SE2	644	0.000	0.88	0.06	0.46	-0.12	-0.97	Same
	SE3	861	0.001	0.11	0.12	0.79	0.31	2.28	Different
	SE4	961	0.001	0.73	0.12	0.84	0.19	1.58	Same
	SE5	648	0.000	0.26	0.02	0.15	0.02	0.13	Same
Exposed	E1	468	0.000	0.15	0.03	0.17	0.03	0.19	Same
	E2	644	NA	NA	NA	NA	NA	NA	NA
	E3	493	NA	NA	NA	NA	NA	NA	NA
	E4	846	0.000	0.75	-0.01	-0.03	-0.03	-0.18	Different
	E5	77	0.000	0.35	-0.01	0.00	-0.04	-0.01	NA

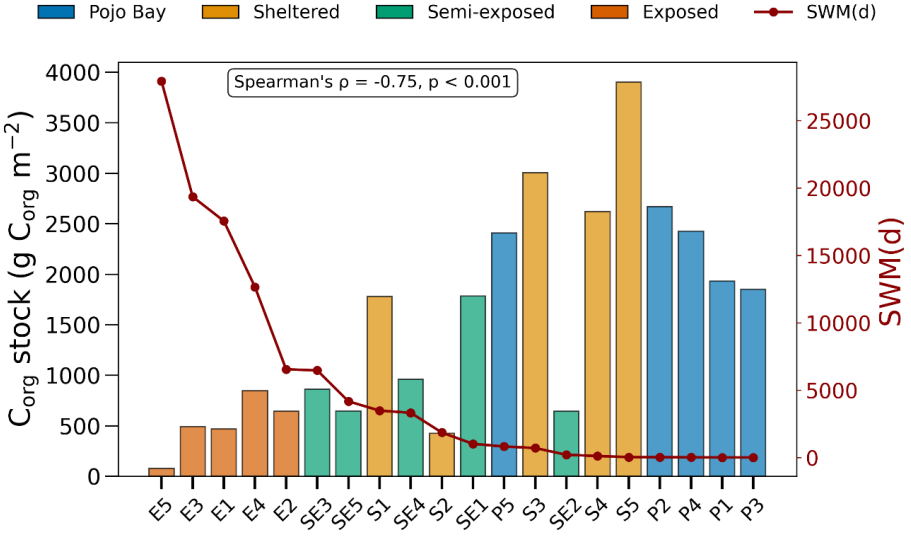

https://doi.org/10.5194/egusphere-2026-4456
Preprint. Discussion started: 5 August 2026

Figure 4: Sedimentary C_{org} stocks and depth-attenuated wave exposure (SWM(d)) across individual sites. Bars represent C_{org} stock, colored by site category, and the red line represents SWM(d) on the secondary y-axis. Sites are ordered by decreasing SWM(d). The textbox/inset shows the Spearman correlation between SWM(d) and C_{org} stock.

5.4 Dissolved constituents and their distribution

The highest average concentrations for DIC, CH_4, NH_4^+, Fe^{2+} and SO_4^{2-} in porewaters were 1.91 ± 0.70 mmol L^{-1} (S4), 0.05±0.03 mmol L^{-1} (P2), 0.37±0.08 mmol L^{-1} (P2), 0.07±0.08 and 0.07 ±0.07 mmol L^{-1} (S4 and S5 respectively) and 5.05±0.14 mmol L^{-1} (SE1) (Table 3). DIC concentrations showed no significant difference among the four categories ($p>0.05$, Table S1, Fig. 5). CH_4 concentrations in Pojo Bay were significantly higher than Semi-exposed and Exposed sites. Moreover, Cliff's delta indicated complete separation, with CH_4 concentration consistently higher in Pojo Bay than in other three categories, driven by the anomalously high concentrations at site P2. For NH_4^+, Pojo Bay and Sheltered categories showed higher values compared to Semi-exposed and Exposed sites but were similar to each other. For Fe^{2+}, values at Exposed sites were close to zero (Fig. 5). However, only Sheltered sites showed a significant difference from Exposed sites, with complete separation of Sheltered Fe^{2+} data shown by Cliff's delta. SO_4^{2-} concentrations showed an increasing trend along the transect from Pojo Bay to Exposed sites, with Exposed sites showing highest porewater concentrations (Table 3).

Table 3: Concentrations of dissolved inorganic carbon (DIC), dissolve methane (CH_4), dissolved ammonium (NH_4^+), dissolved iron (II) (Fe^{2+}) and dissolved sulfate (SO_4^{2-}) in bottom water (BW) and average of sediment porewater (PW) for each site. NA (not available)

Category	Sites	DIC (mmol L^{-1})		CH_4 (mmol L^{-1})		NH_4^+ (mmol L^{-1})		Fe^{2+} (mmol L^{-1})		SO_4^{2-} (mmol L^{-1})	
		BW	PW (Mean ±SD)	BW	PW (Mean ±SD)	BW	PW (Mean ±SD)	BW	PW (Mean ±SD)	BW	PW (Mean ±SD)
Pojo Bay	P1	0.41	1.08±0.29	0.00	0.00±0.01	0.01	0.10±0.03	0.00	0.03±0.04	1.31	0.82±0.16
	P2	0.58	1.51±0.47	0.00	0.05±0.03	0.01	0.37±0.08	0.00	0.00±0.01	1.36	0.50±0.33
	P3	0.81	0.59±0.08	0.00	0.00±0.00	0.00	0.07±0.01	0.00	0.01±0.02	1.89	2.41±0.14
	P4	0.72	0.75±0.18	0.00	0.00±0.00	0.00	0.08±0.05	0.00	0.05±0.06	2.68	2.81±0.15
Sheltered	S1	0.40	0.52±0.26	0.00	0.00±0.00	0.01	0.09±0.02	0.00	0.02±0.02	4.18	2.83±2.04
	S2	1.21	1.38±0.56	0.00	0.00±0.00	0.01	0.08±0.02	0.00	0.04±0.03	4.22	4.12±0.20
	S3	0.53	1.36±0.31	0.00	0.00±0.00	0.01	0.13±0.02	0.00	0.03±0.05	4.50	4.07±2.19
	S4	1.32	1.91±0.70	0.00	0.00±0.00	0.01	0.16±0.04	0.00	0.07±0.07	4.28	2.56±1.40
	S5	NA	1.50±0.52	NA	0.00±0.00	NA	0.14±0.07	NA	0.07±0.08	NA	3.19±1.22
Semi-exposed	SE1	0.60	1.25±0.66	0.00	0.00±0.00	0.01	0.04±0.01	0.00	0.01±0.01	5.19	5.05±0.14
	SE2	0.67	0.94±0.19	0.00	0.00±0.00	0.00	0.05±0.02	0.00	0.00±0.00	4.61	4.59±0.21
	SE3	1.03	1.17±0.34	0.00	0.00±0.00	0.05	0.05±0.02	0.00	0.04±0.03	4.69	4.39±0.10

https://doi.org/10.5194/egusphere-2026-4456
Preprint. Discussion started: 5 August 2026

	SE4	0.77	0.86±0.08	0.00	0.00±0.00	0.01	0.07±0.01	0.00	0.03±0.03	4.66	4.33±0.12
	SE5	0.72	0.90±0.12	0.00	0.00±0.00	0.00	0.02±0.01	0.00	0.01±0.01	4.50	4.20±0.13
Exposed	E1	1.17	1.18±0.63	0.00	0.00±0.00	0.01	0.03±0.01	0.00	0.00±0.00	5.46	4.75±1.12
	E4	1.02	1.00±0.27	0.00	0.00±0.00	0.00	0.01±0.01	0.00	0.00±0.00	5.06	5.04±0.05
	E5	0.97	0.87±0.34	0.00	0.00±0.00	0.00	0.01±0.00	0.00	0.00±0.00	4.81	5.01±0.15

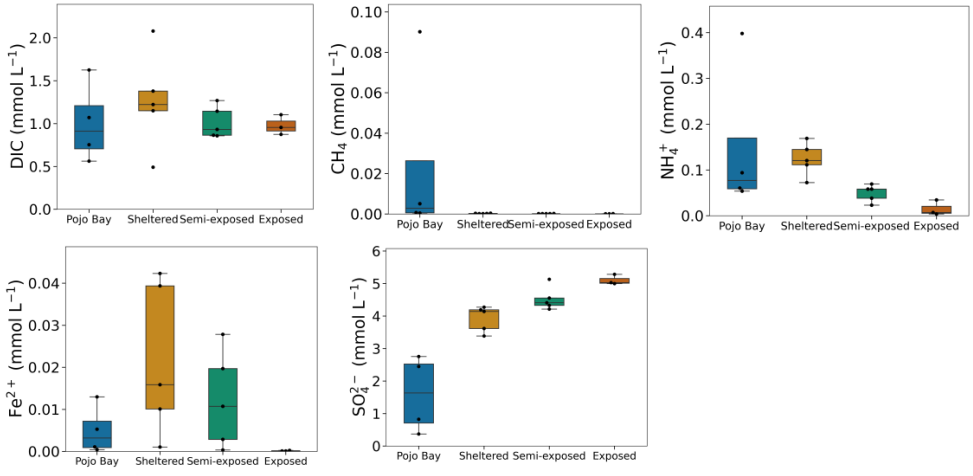

Figure 5: Porewater distribution (median) of dissolved inorganic carbon (DIC), dissolved methane (CH_4), dissolved ammonium (NH_4^+), dissolved iron (II) (Fe^{2+}) and SO_4^{2-} in mmol L^{-1} on y-axis with category on x-axis. For statistical test results, see Table S1.

5.5 Estimates of diffusive fluxes and turnover rates

Overall, DIC fluxes across the sediment-water interface were relatively high in Pojo Bay and Sheltered sites, ranging from -1.41 to26.81 mmol m^{-2} d^{-1} (Fig. 6, Table 2). Semi-exposed and Exposed sites showed relatively lower rates from -0.97 to 2.28 mmol m^{-2} d^{-1}, of which Exposed sites did not exceed more than 1 mmol m^{-2} d^{-1} (Table 2). Spearman's rank analysis showed positive monotonic correlation between absolute DIC fluxes (estimated from the median of DS1, DS2 and DS3 methods) and the sediment C_{org} stock of the top 10 cm, with Spearman's $\rho = 0.738$ and $p < 0.05$ (Table S2). The highest DIC fluxes were observed at site P2, ranging from 10.07 to 26.81 mmol m^{-2} d^{-1} from the DS1, DS2 and DS3 estimates. The CH_4 flux across the sediment-water interface was highest at site P2, at 0.32 mmol m^{-2} d^{-1} (Table 2). However, CH_4 accounted for a negligible fraction of the dissolved carbon flux with values several orders of magnitude lower than for DIC.

https://doi.org/10.5194/egusphere-2026-4456
Preprint. Discussion started: 5 August 2026

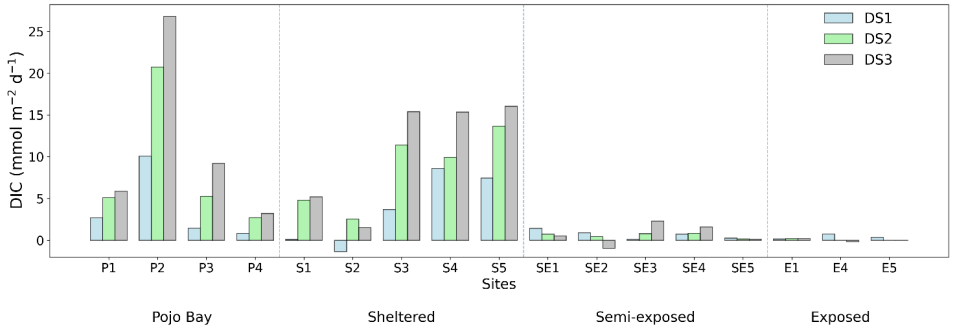

Figure 6: DIC (dissolved inorganic carbon) fluxes for individual sites grouped by category. Blue, green, and grey bars represent DS1, DS2, and DS3, respectively (described in section 3.3). The y-axis shows DIC flux in mmol m^{-2} d^{-1}, and the x-axis shows sites within each category.

When reported as % turnover of the C_{org} stock in the uppermost 10 cm of the sediment column, all categories of sites showed generally low values of <14% turnover in one annual cycle (Fig. 7). Turnover was highest at site P2, with 13.33 % turnover estimated through the DS3 approach. Median turnover (% yr^{-1}) showed a significant positive monotonic relation with the magnitude of the C_{org} stock (Fig. 7), with higher fractional turnover observed at Pojo Bay and Sheltered sites compared to Exposed and Semi-Exposed sites.

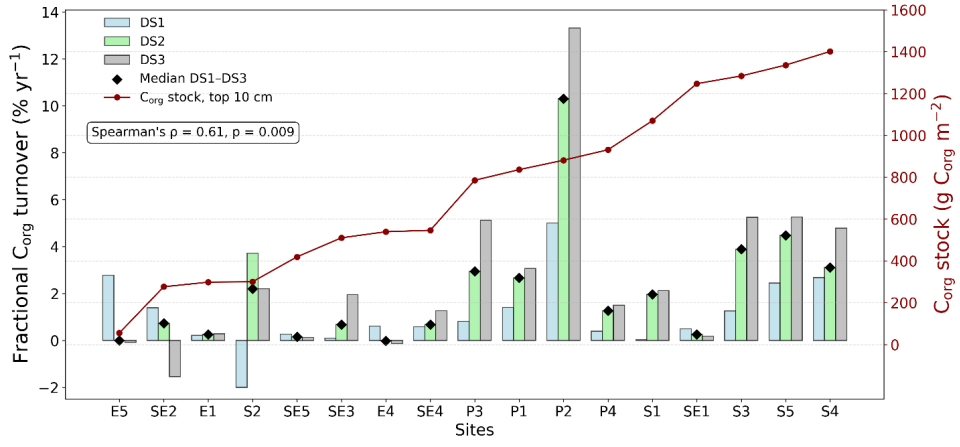

Figure 7: Fractional C_{org} turnover (left y-axis) estimated from three flux approaches (DS1–DS3) across sites arranged by increasing top 10 cm C_{org} stock. Bars show turnover estimates from DS1, DS2, and DS3; black diamonds show the site-level median across DS1–DS3 used for Spearman correlation test. The red line indicates top 10cm C_{org} stock plotted on the secondary y-axis. The inset reports the Spearman correlation between top-10-cm C_{org}.

6. Discussion

6.1 Influence of wave exposure on sediment properties and standing carbon stocks

Seafloor topography showed a great influence on the physical and chemical characteristics of the sediments. The positive monotonic relationship between grain size (D50) and SWM(d) reflects the fact that increasing wave

https://doi.org/10.5194/egusphere-2026-4456
Preprint. Discussion started: 5 August 2026

energy preferentially removes fine particles, resulting in coarser sediments in exposed environments. This natural hydrodynamic sorting mechanism also favors accumulation of organic matter in more sheltered locations, due to sorptive preservation of organic compounds on the higher-surface area minerogenic fraction (Keil et al., 1994; Keil and Cowie, 1999) and the fine particulate nature of diffuse OM. The average mud content (silt + clay, <63 µm) was >50% in Pojo Bay and Sheltered sites. However, cores from some anomalous locations (e.g. S1, S2) showed high mud content but low carbon stocks. These sites were characterized by very low C_{org} overall, declining rapidly below the sediment-water interface (Fig. S1), and appeared generally light-colored, consistent with postglacial clay sediments influenced by redeposition of older, organic-poor sediments (Winterhalter, 1992) that are typical for coastal environments of the northern Baltic Sea (Virtasalo et al., 2007). This observation highlights that SWM(d) does not entirely capture local variability of the seafloor environment that may influence OM accumulation. Other factors may include the effects of small-scale seafloor morphology such as slope angle, effects of currents and resuspension potential. Also, in shallow areas, habitat patchiness and biological activity may regulate the retention or removal of organic matter. Joensuu et al. (2018) showed that biota can explain a substantial proportion of variability in resuspension. Vegetation, macrofauna and biofilms can modify sediment stability and erosion thresholds, allowing fine material to accumulate in certain locations while promoting resuspension and removal in others.

6.2 Comparison of carbon stock data with earlier studies

The average carbon stock in the upper 25 cm was 1522 ± 1061 g C m^{-2}, placing the study area within the broad range reported for shallow near-shore Baltic environments, including seagrass-associated sediments and shallow enclosed coastal bays (Gubri et al., 2025; Röhr et al., 2016; Wikström et al., 2025). Notably, our dataset spans an estuary–archipelago exposure gradient from sheltered depositional areas to exposed sandy sites. This distinction is important when comparing with Gubri et al.(2025) who reported a higher mean stock of 2561 ± 81 g C m^{-2} but studied exclusively shallow enclosed bays, a more morphometrically restricted and sheltered habitat type than the full gradient covered in our study. The large variability among sites therefore reflects strong spatial heterogeneity in sedimentary OM retention. Across the range of C_{org} stock, low C_{org} stocks in the Exposed sites were comparable to values reported for Finnish eelgrass habitats, where strong hydrodynamic forcing can limit local OM retention and promote export to deeper or more sheltered depositional areas(Röhr et al., 2016). At the higher end of estimated C_{org} stocks, values exceeded those reported for Baltic eelgrass meadows and temperate seagrass regions (Billman et al., 2023; Röhr et al., 2018). Overall, this comparison shows that the wide range of C_{org} stocks in the study area is primarily linked to spatial variation in hydrodynamic exposure and depositional setting as well as a broad range of habitats along the salinity gradient. This emphasizes the need to distinguish localized shallow-water carbon storage from broader coastal or basin-scale stock averages, such as the Baltic Sea baseline of 830 ± 90 g C m^{-2} reported mainly for deeper open-sea sediments (Scheffold and Hense, 2020).

6.3 Reactivity and turnover of the carbon stock

6.3.1 General interpretation of porewater parameters

Of the measured porewater parameters, NH_4^+ may be considered the best indicator of OM remineralization. Because the concentration of NH_4^+ in the bottom water is low, in situ production in the sediment can be clearly observed through concentration gradients in the porewaters. DIC also reflects remineralization, however, its

https://doi.org/10.5194/egusphere-2026-4456
Preprint. Discussion started: 5 August 2026

concentration along the study transect is also positively influenced by the salinity gradient (Geilfus et al., 2026), and its distribution must be interpreted more cautiously. SO_4^{2-} concentrations are also directly associated with salinity, indicated by the increasing trend along the transect. CH_4 and Fe^{2+} are primarily controlled by the redox zonation, with their concentrations reflecting the progression of anaerobic diagenetic processes below the sediment-water interface. The observed redox zonation in porewaters at our study sites is generally as expected for brackish marine environments. Most of the porewater profiles showed a clear peak of Fe^{2+} (Fig. S2), reflecting the Fe oxide reduction zone in the uppermost 25 cm of the sediment core. This peak in Fe^{2+}, however, was completely absent in the Exposed sites, reflecting the low sediment OM content and consequent weakening of iron reduction within the sediment column. We also observed a strong compression of the redox zones at site P2, with high OM% and shallow penetration of SO_4^{2-} in the low-salinity Pojo Bay (Jilbert et al., 2018). This led to the anomalous presence of relatively high CH_4 concentrations in the uppermost 25 cm of the sediments.

6.3.2 Magnitude of remineralization in sediments

Overall, porewater NH_4^+ showed highest concentrations in Pojo Bay and Sheltered sites (Fig. 5). Consequently, the NH_4^+-derived fluxes of DIC from method DS2 were also higher at these sites (Fig. 6). Combined, these results indicate higher absolute remineralisation rates, consistent with the interpretation that OM availability regulates spatial variability in remineralization (Srithongouthai and Tada, 2015). The magnitude of NH_4^+ and DIC fluxes observed in our study are broadly comparable to the deeper sediment diffusion fluxes in the Baltic Sea (Jilbert et al., 2011; Lengier et al., 2021). The ranges of observed values both in the near-shore environments of this study (-0.12 to 2.84 mmol m^{-2} d^{-1} for NH_4^+ and -1.37 to 26.81 mmol m^{-2} d^{-1} for DIC) and deeper areas of the Baltic Sea (0.04 to 1.37 mmol m^{-2} d^{-1} for NH_4^+, -0.01 to 3.33 mmol m^{-2} d^{-1} for DIC by Lengier et al. (2021)are wide, indicating a diversity of conditions in both cases. However, the high maximum values in our results highlight that near-shore sedimentary environments are important loci for processing of carbon, potentially exceeding the regional benchmarks of benthic diffusive fluxes in the deeper areas of the Baltic Sea.

Estimated DIC fluxes from the three separate calculation approaches yielded values mostly in the same order of magnitude (Fig. 6, Table 2). This consistency is important, suggesting that the porewater data can be used to model a steady-state mass balance where internal production of DIC in the sediment column through remineralization is balanced by the exchange across the sediment-water interface. Values of DS1 and DS2 are expected to be comparable because they are both derived from the exchange at SWI. Differences between DS1 and DS2 could arise from uncertainty in the assumptions used in NH_4^+-based DIC fluxes, which include the diffusive coefficient and the C/N stoichiometry of the degrading OM (Arndt et al., 2013). Poor control on the stoichiometry could arise due to alteration of C/N ratios during early diagenesis by selective degradation and from the possibility that the degrading fractions of OM have a different C/N ratio from the bulk value (Arndt et al., 2013; Freudenthal et al., 2001). In this study, DIC fluxes in sites in Pojo Bay by methods DS2 and DS3 could be overestimated if the degrading material had a significantly lower C/N than the bulk sediment value used in the estimation of DIC fluxes based on NH_4^+. This could explain, for example, the higher DS2 and DS3-estimated DIC fluxes relative to DS1-estimated value at site P2 (Fig. 6). Values for DS3 are derived from the whole sediment profile and integrate the production and consumption processes over a larger depth interval which are not expressed in DS1 and DS2. Thus, some differences between DS3 and the other two approaches may be expected, as observed in the outputs.

https://doi.org/10.5194/egusphere-2026-4456
Preprint. Discussion started: 5 August 2026

6.3.3 Fractional turnover of the carbon stock

The fractional turnover of the uppermost 10 cm of the standing carbon stock estimated from the three approaches was generally low. Across all sites, flux-derived annual fractional turnover remained below 14% yr^{-1}. Maximum values were observed at site P2, where the DS3 calculation estimated a turnover of 13.33% yr^{-1}. Overall, the estimates suggest that only a small fraction of standing carbon stock is being remineralized on an annual basis along the transect.

Median estimates of fractional turnover (from DS1, DS2 and DS3) showed a significant positive monotonic relationship with top 10 cm carbon stock across all sites (Spearman $\rho = 0.61$, $p < 0.05$; Fig. 7), implying proportionally more active turnover at more carbon-rich sites. To assess the extent to which variable sources of sediment OM might influence overall reactivity, we tested the significance of the relationship between bulk C/N ratio and median fractional turnover. We hypothesized that sediments of higher bulk C/N should display lower fractional turnover due to the dominance of low-reactivity, terrestrial-derived OM. In practice therefore, we expected to observe lowest fractional turnover at the Pojo Bay sites with relatively high C/N and low $\delta^{13}C$ (Fig. 2), indicative of predominantly terrestrial OM. However, contrary to this expectation, C/N showed a moderate positive rank association with fractional turnover (Fig. 8). Bulk C/N and $\delta^{13}C$ integrate the composition of the whole sedimentary organic-matter pool, whereas porewater fluxes reflect the fraction of OM which is actively remineralized over much shorter timescales. Therefore, the significant relationship may reflect subtle spatial differences in the amount of labile OM, rather than a direct effect of bulk OM quality. In this context, Pojo Bay and Sheltered sites are known to receive phytoplankton-derived autochthonous OM under eutrophied conditions (Jilbert et al., 2018). This relatively labile OM can be rapidly remineralized, producing porewater solutes such as DIC and NH_4^+, leading to steep concentration gradients and higher calculated diffusive fluxes. In addition, nearby macrophyte-derived OM may contribute labile autochthonous material at these shallow sampling depths, further supporting rapid remineralisation (Lammerant et al., 2025). Site P2 shows the highest DIC and NH_4^+ fluxes in the study area despite the influence of terrestrial OM in the bulk sediment composition (Figs. 2 and 6). This result again highlights the possibility that specific fractions of the bulk sedimentary organic matter may be responsible for the regeneration of carbon and nutrients due to relatively rapid degradation rates. At site P2, the sediment surface was covered by filamentous green algae during sampling, which may have contributed to the anomalous porewater chemistry at this site.

https://doi.org/10.5194/egusphere-2026-4456
Preprint. Discussion started: 5 August 2026

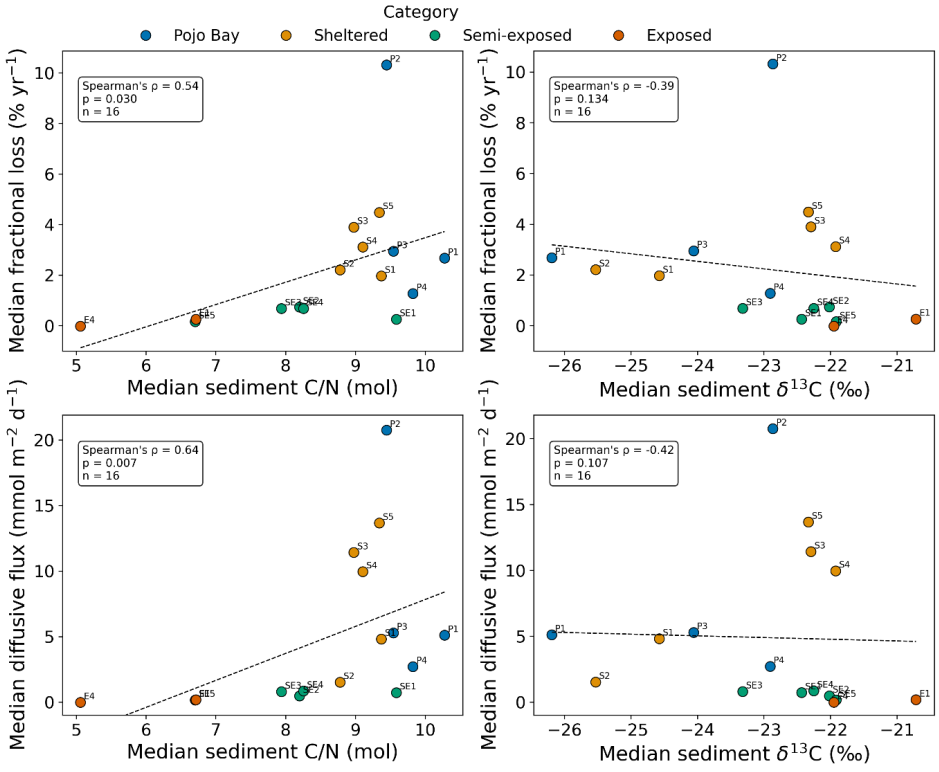

Figure 8. Relationships between bulk sediment organic-matter indicators and carbon-processing metrics. Median fractional carbon loss (% yr^{-1}) and median diffusive flux (mmol m^{-2} d^{-1}) plotted against median sediment C/N and bulk sediment δ^{13}C (‰). Points represent individual sites and are coloured by site category. Site codes are shown beside each point. Dashed lines indicate linear fits for visual guidance only. Spearman's ρ, p-value, and sample size are displayed in each correlation, significance valid if p < 0.05. The δ^{13}C (‰) value for site E3 is assumed equivalent to that of the E4 site and E5 was excluded from the correlation test.

Uncertainty in the individual flux estimates, and thus the fractional turnover, is potentially derived from the presence of infauna (Kristensen, 2000). The outer archipelago, with sandy to mixed sediments, hosts diverse benthic communities (Villnäs et al., 2019) with key species such as *Macoma balthica, Cerastoderma glaucum, Hediste diversicolor, and Marenzelleria* spp. Gammal et al. (2025) observed that in shallow coastal habitats (<4 m) *Macoma balthica* and *Cerastoderma glaucum* affect mineralization rates both through their metabolism and sediment reworking modes. *Macoma balthica* and *Cerastoderma glaucum* mainly affect the sediments through shallow bioturbation/biodiffusion, while species such as *Hediste diversicolor* and *Marenzelleria* spp. have stronger effects through burrow construction and bioirrigation, enhancing non-diffusive solute transport in porewaters. Benthic faunal respiration has been estimated to mineralize 8–17 g C m^{-2} yr^{-1}, corresponding to 22–31% of C_{org} input to Baltic sediments (Ehrnsten et al., 2022), while in the Gulf of Finland, macrofauna are estimated to contribute 18–26% of total benthic respiration in soft-bottom sites and 11–45% in hard-bottom sites (Rodil et al., 2019) Importantly, faunal bioturbation and -irrigation rates, and thus their impact on sediment solute concentration and fluxes is shown to differ with sediment type and other habitat characteristics, complicating

https://doi.org/10.5194/egusphere-2026-4456
Preprint. Discussion started: 5 August 2026

estimations of their effects across heterogeneous coastal habitats (Bernard et al., 2019; Gammal et al., 2019). Consequently, when estimating fluxes using DS3, multiple zones of production and consumption were observed in modelled profiles (Fig. S3), likely partly reflecting the effect of infaunal processes on the porewater data. Since the PROFILE model was implemented with bioturbation and bioirrigation coefficients set to zero, the transport effect of infauna was nominally incorporated into the calculated net reaction (R). Notably, site P2 showed more classic porewater profiles indicative of steady-state diagenesis (e.g., Berg et al., 1998; Schulz, 2006) and was also characterized by low infaunal activity (Janina Pykäri, personal communication), supporting the interpretation that porewater profiles of other sites may have been influenced by disturbance due to infauna.

Another factor that may have influenced the overall exchange of carbon at the sediment-water interface was advective transport through resuspension, which is likely to be important in parts of the study area, especially in Semi-exposed and Exposed sandy sediments. Wave-driven resuspension and intermittent porewater flushing have been shown to enhance NH_4^+ exchange in the same Semi-exposed sites (Niemistö and Lund-Hansen, 2019). These processes cannot be captured by our sampling approach but may add to the overall mobilization of dissolved carbon and nutrients to the water column.

7. Conclusions

To conclude, this study contributes to our understanding of sedimentary carbon storage and remineralisation in shallow nearshore sediments across a heterogeneous coastal gradient. Sedimentary C_{org} stocks varied strongly over short spatial scales and decreased with increasing depth-attenuated wave exposure. Together with the strong relationship between D50 and mud-sized fraction, this pattern is consistent with hydrodynamic sorting and fine-sediment retention as important controls on carbon accumulation. Sheltered and estuarine depositional settings generally supported higher C_{org} stocks, highlighting the importance of low-exposure areas for nearshore carbon storage.

However, sediment texture alone did not explain the full spatial variability. The occurrence of mud-rich but low-C_{org} sites indicates that local depositional history, sediment origin, organic-matter supply, mineral dilution, and degradation may also influence carbon accumulation. This shows that high mud content does not necessarily imply high C_{org} storage, even though fine-grained sediments generally provide favourable conditions for organic-matter retention.

Diffusive fluxes and flux-derived turnover estimates showed that these sediments were not only carbon storage environments but also active sites of remineralisation. Fractional turnover was generally low on an annual basis, with a maximum of approximately 14% yr^{-1} of the standing C_{org} stock, indicating that most of the sedimentary C_{org} pool was retained. Sheltered, fine-grained sediments therefore represent important nearshore carbon-storage areas, although their long-term sequestration potential cannot be resolved without sediment accumulation or burial rate estimates. Overall, the results highlight the need to evaluate shallow coastal C_{org} stocks together with remineralisation when assessing carbon retention in heterogeneous nearshore environments.

Data availability

The data supporting this study is available from Zenodo (Nishant et al., 2026): https://doi.org/10.5281/zenodo.21512381

https://doi.org/10.5194/egusphere-2026-4456
Preprint. Discussion started: 5 August 2026

Supplement

Supplemental material is supplied as a separate file.

Author contributions

NN performed the measurements, data curation, visualisation and wrote the manuscript draft; JP and RL contributed with sample collection; AV, CG, AN, TJ planning and contributed with sample collection with field campaign. TJ and GC supervised the work. All the authors reviewed and edited the manuscript.

Competing interests

The authors declare no conflict of interest.

Acknowledgements

The work is supported by Walter and Andrée de Nottbeck foundation (NN, JP, RL), the Jane and Aatos Erkko Foundation (AN, CG), Sophie von Julins Foundation (AN, AV) and utilizes the research infrastructure facilities at Tvärminne Zoological Station, University of Helsinki, as part of FINMARI (Finnish Marine Research Infrastructure Consortium), along with the laboratory infrastructure provided by Hellabs at the Department of Geosciences and Geography, University of Helsinki. Additionally, facilities at University of Jyväskylä were utilised. This is a publication from the Centre for Coastal Ecosystem and Climate Change Research (www.coastclim.org) and Hellabs publication #45. The work also acknowledges the help provided by Max O. A. Kankainen and Ana Lúcia Lindroth Dauner with sample processing and data handling. Anna-Roosa Vesanen and Jenna Hölttä for their help in the field, and Juhani Virkanen, Hanna Reijola and Tuija Vaahtojärvi for assistance in the laboratory. AI tool was used for limited debugging of python code and aesthetic adjustments of plots through the code.

Financial support

The work has been supported by the Walter ja Andrée de Nottbeckin Säätiö (grant nos. 20260041, 20250019). Open-access funding was provided by the Helsinki University Library.

References

Alenius, P., Myrberg, K., and Nekrasov, A.: The physical oceanography of the Gulf of Finland: a review, Boreal Environ. Res., 3, 97–125, 1998.

Arndt, S., Jørgensen, B. B., LaRowe, D. E., Middelburg, J. J., Pancost, R. D., and Regnier, P.: Quantifying the degradation of organic matter in marine sediments: A review and synthesis, Earth-Sci. Rev., 123, 53–86, https://doi.org/10.1016/j.earscirev.2013.02.008, 2013.

Asmala, E., Kaartokallio, H., Carstensen, J., and Thomas, D. N.: Variation in riverine inputs affect dissolved organic matter characteristics throughout the estuarine gradient, Front. Mar. Sci., 2, https://doi.org/10.3389/fmars.2015.00125, 2016.

Attard, K. M., Rodil, I. F., Glud, R. N., Berg, P., Norkko, J., and Norkko, A.: Seasonal ecosystem metabolism across shallow benthic habitats measured by aquatic eddy covariance, Limnol. Oceanogr. Lett., 4, 79–86, https://doi.org/10.1002/lol2.10107, 2019.

https://doi.org/10.5194/egusphere-2026-4456
Preprint. Discussion started: 5 August 2026

Atwood, T. B., Witt, A., Mayorga, J., Hammill, E., and Sala, E.: Global Patterns in Marine Sediment Carbon Stocks, Front. Mar. Sci., 7, https://doi.org/10.3389/fmars.2020.00165, 2020.

Bauer, J. E., Cai, W. J., Raymond, P. A., Bianchi, T. S., Hopkinson, C. S., and Regnier, P. A. G.: The changing carbon cycle of the coastal ocean, Nature, 504, 61–70, https://doi.org/10.1038/nature12857, 2013.

Berg, P., Risgaard-Petersen, N., and Rysgaard, S.: Interpretation of measured concentration profiles in sediment pore water, Limnol. Oceanogr., 43, 1500–1510, https://doi.org/10.4319/lo.1998.43.7.1500, 1998.

Bernard, G., Gammal, J., Järnström, M., Norkko, J., and Norkko, A.: Quantifying bioturbation across coastal seascapes: Habitat characteristics modify effects of macrofaunal communities, J. Sea Res., 152, 101766, https://doi.org/10.1016/J.SEARES.2019.101766, 2019.

Berner, R. A.: Early Diagenesis: A Theoretical Approach, Princeton University Press, Princeton, New Jersey, 1980.

Billman, M., Santos, I. R., and Jahnke, M.: Small carbon stocks in sediments of Baltic Sea eelgrass meadows, Front. Mar. Sci., 10, https://doi.org/10.3389/fmars.2023.1219708, 2023.

Boudreau, B. P.: Diagenetic Models and Their Implementation Modelling Transport and Reactions in Aquatic Sediments, Springer, Berlin, 1997.

Burdige, D. J.: Physical properties of sediments, in: Geochemistry of Marine Sediments, Princeton University Press, Princeton, 2006.

Burdige, D. J.: Preservation of organic matter in marine sediments: Controls, mechanisms, and an imbalance in sediment organic carbon budgets?, Chem. Rev., 107, 467–485, https://doi.org/10.1021/cr050347q, 2007.

Carstensen, J., Conley, D. J., Bonsdorff, E., Gustafsson, B. G., Hietanen, S., Janas, U., Jilbert, T., Maximov, A., Norkko, A., Norkko, J., Reed, D. C., Slomp, C. P., Timmermann, K., and Voss, M.: Hypoxia in the Baltic Sea: Biogeochemical cycles, benthic fauna, and management, Ambio, 43, 26–36, https://doi.org/10.1007/s13280-013-0474-7, 2014.

Chatting, M., Diesing, M., Hunter, W. R., Grey, A., Kelleher, B. P., and Coughlan, M.: Improving marine sediment carbon stock estimates: the role of dry bulk density and predictor adjustments, Biogeosciences, 22, 5975–5990, https://doi.org/10.5194/bg-22-5975-2025, 2025.

Chen, S., Yao, P., Wang, Z., Zhao, B., Wang, L., Han, L., Wang, N., Ye, X., and Gao, C.: Thermal stability of sedimentary organic carbon in a large river dominated marginal sea, Science of the Total Environment, 954, https://doi.org/10.1016/j.scitotenv.2024.176570, 2024.

Conley, D. J., Carstensen, J., Aigars, J., Axe, P., Bonsdorff, E., Eremina, T., Haahti, B. M., Humborg, C., Jonsson, P., Kotta, J., Lännegren, C., Larsson, U., Maximov, A., Medina, M. R., Lysiak-Pastuszak, E., Remeikaitè-Nikienè, N., Walve, J., Wilhelms, S., and Zillén, L.: Hypoxia is increasing in the coastal zone of the baltic sea, Environ. Sci. Technol., 45, 6777–6783, https://doi.org/10.1021/es201212r, 2011.

https://doi.org/10.5194/egusphere-2026-4456
Preprint. Discussion started: 5 August 2026

Duarte, C. M., Middelburg, J. J., and Caraco, N.: Major role of marine vegetation on the oceanic carbon cycle, Biogeosciences, 2, 1–8, https://doi.org/10.5194/bg-2-1-2005, 2005.

Ehrnsten, E., Pavlovitch Savchuk, O., and Gustafsson, B. G.: Modelling the effects of benthic fauna on carbon, nitrogen and phosphorus dynamics in the Baltic Sea, Biogeosciences, 19, 3337–3367, https://doi.org/10.5194/bg-19-3337-2022, 2022.

Freudenthal, T., Wagner, T., Wenzhöfer, F., Zabel, M., and Wefer, G.: Early diagenesis of organic matter from sediments of the eastern subtropical Atlantic: evidence from stable nitrogen and carbon isotopes, Geochim. Cosmochim. Acta, 65, 1795–1808, https://doi.org/10.1016/S0016-7037(01)00554-3, 2001.

Gammal, J., Järnström, M., Bernard, G., Norkko, J., and Norkko, A.: Environmental Context Mediates Biodiversity–Ecosystem Functioning Relationships in Coastal Soft-sediment Habitats, Ecosystems, 22, 137–151, https://doi.org/10.1007/S10021-018-0258-9, 2019.

Gammal, J., Järnström, M., Norkko, J., Bonsdorff, E., and Norkko, A.: Seasonal Variation in the Role of Benthic Macrofauna Communities for Ecosystem Functioning in Shallow Coastal Soft-Sediment Habitats, Estuaries and Coasts, 48, https://doi.org/10.1007/s12237-025-01499-z, 2025.

Geilfus, N. X., Delille, B., Villnäs, A., and Norkko, A.: Spatial heterogeneity of GHG dynamics across an estuarine ecosystem, Biogeosciences, 23, 1931–1948, https://doi.org/10.5194/bg-23-1931-2026, 2026.

Gubri, B., Hansen, J. P., Wikström, S. A., Snickars, M., Dahl, M., Gullström, M., Rydin, E., Masqué, P., Garbaras, A., Björk, M., and Boström, C.: Shallow Coastal Bays as Sediment Carbon and Nutrient Reservoirs in the Baltic Sea, Estuaries and Coasts, 48, https://doi.org/10.1007/s12237-025-01541-0, 2025.

Gustafsson, B. G., Schenk, F., Blenckner, T., Eilola, K., Meier, H. E. M., Müller-Karulis, B., Neumann, T., Ruoho-Airola, T., Savchuk, O. P., and Zorita, E.: Reconstructing the development of baltic sea eutrophication 1850-2006, Ambio, 41, 534–548, https://doi.org/10.1007/s13280-012-0318-x, 2012.

Hedges, J. I. and Keil, R. G.: Sedimentary organic matter preservation: an assessment and speculative synthesis, Mar. Chem., 49, 81–115, https://doi.org/10.1016/0304-4203(95)00008-F, 1995.

Hemingway, J. D., Rothman, D. H., Rosengard, S. Z., and Galy, V. V.: Technical note: An inverse method to relate organic carbon reactivity to isotope composition from serial oxidation, Biogeosciences, 14, 5099–5114, https://doi.org/10.5194/bg-14-5099-2017, 2017.

Jilbert, T., Slomp, C. P., Gustafsson, B. G., and Boer, W.: Beyond the Fe-P-redox connection: Preferential regeneration of phosphorus from organic matter as a key control on Baltic Sea nutrient cycles, Biogeosciences, 8, 1699–1720, https://doi.org/10.5194/bg-8-1699-2011, 2011.

Jilbert, T., Asmala, E., Schröder, C., Tiihonen, R., Myllykangas, J. P., Virtasalo, J. J., Kotilainen, A., Peltola, P., Ekholm, P., and Hietanen, S.: Impacts of flocculation on the distribution and diagenesis of iron in boreal estuarine sediments, Biogeosciences, 15, 1243–1271, https://doi.org/10.5194/bg-15-1243-2018, 2018.

Jilbert, T., Jokinen, S., Saarinen, T., Mattus-Kumpunen, U., Simojoki, A., Saarni, S., Salminen, S., Niemistö, J., and Horppila, J.: Impacts of a deep reactive layer on sedimentary phosphorus dynamics in a boreal lake

https://doi.org/10.5194/egusphere-2026-4456
Preprint. Discussion started: 5 August 2026

recovering from eutrophication, Hydrobiologia, 847, 4401–4423, https://doi.org/10.1007/s10750-020-04289-9, 2020.

Jilbert, T., Cowie, G., Lintumäki, L., Jokinen, S., Asmala, E., Sun, X., Mörth, C. M., Norkko, A., and Humborg, C.: Anthropogenic Inputs of Terrestrial Organic Matter Influence Carbon Loading and Methanogenesis in Coastal Baltic Sea Sediments, Front. Earth Sci. (Lausanne)., 9, https://doi.org/10.3389/feart.2021.716416, 2021.

Joensuu, M., Pilditch, C. A., Harris, R., Hietanen, S., Pettersson, H., and Norkko, A.: Sediment properties, biota, and local habitat structure explain variation in the erodibility of coastal sediments, Limnol. Oceanogr., 63, 173–186, https://doi.org/10.1002/lno.10622, 2018.

Keil, R. G. and Cowie, G. L.: Organic matter preservation through the oxygen-deficient zone of the NE Arabian Sea as discerned by organic carbon:mineral surface area ratios, Mar. Geol., 161, 13–22, https://doi.org/10.1016/S0025-3227(99)00052-3, 1999.

Keil, R. G., Tsamakis, E., Fuh, C. B., Calvin Giddings, J., and Hedges', J. 1: Mineralogical and textural controls on the organic composition of coastal marine sediments: Hydrodynamic separation using SPLITT-fractionation, Geochim. Cosmochim. Acta, 58, 879–893, https://doi.org/10.1016/0016-7037(94)90512-6, 1994.

Kristensen, E.: Organic matter diagenesis at the oxic/anoxic interface in coastal marine sediments, with emphasis on the role of burrowing animals, Hydrobiologia, 426, 1–24, https://doi.org/10.1023/A:1003980226194, 2000.

Kristensen, E., Penha-Lopes, G., Delefosse, M., Valdemarsen, T., Quintana, C. O., and Banta, G. T.: What is bioturbation? the need for a precise definition for fauna in aquatic sciences, Mar. Ecol. Prog. Ser., 446, 285–302, https://doi.org/10.3354/meps09506, 2012.

Kuliński, K., Rehder, G., Asmala, E., Bartosova, A., Carstensen, J., Gustafsson, B., Hall, P. O. J., Humborg, C., Jilbert, T., Jürgens, K., Meier, H. E. M., Müller-Karulis, B., Naumann, M., Olesen, J. E., Savchuk, O., Schramm, A., Slomp, C. P., Sofiev, M., Sobek, A., Szymczycha, B., and Undeman, E.: Biogeochemical functioning of the Baltic Sea, Earth System Dynamics, 13, 633–685, https://doi.org/10.5194/esd-13-633-2022, 2022.

Lammerant, R., Hölttä, J., Pykäri, J., Nishant, N., Villnäs, A., Wikström, S. A., Norkko, A., and Gustafsson, C.: Environmental gradients strongly affect functional composition and biomass C stocks within aquatic plant meadows, Ecosphere, 16, https://doi.org/10.1002/ecs2.70327, 2025.

Lengier, M., Szymczycha, B., Brodecka-Goluch, A., Kłostowska, Ż., and Kuliński, K.: Benthic diffusive fluxes of organic and inorganic carbon, ammonium and phosphates from deep water sediments of the Baltic Sea, Oceanologia, 63, 370–384, https://doi.org/10.1016/j.oceano.2021.04.002, 2021.

Lindroth Dauner, A. L., Kankainen, M. O. A., Väkevä, S., Asmala, E., Järvinen, M., Koho, K., and Jilbert, T.: Shoreline exposure controls teal carbon accumulation in boreal lakes, Biogeosciences, 23, 3637–3653, https://doi.org/10.5194/BG-23-3637-2026, 2026.

Macreadie, P. I., Anton, A., Raven, J. A., Beaumont, N., Connolly, R. M., Friess, D. A., Kelleway, J. J., Kennedy, H., Kuwae, T., Lavery, P. S., Lovelock, C. E., Smale, D. A., Apostolaki, E. T., Atwood, T. B., Baldock,

https://doi.org/10.5194/egusphere-2026-4456
Preprint. Discussion started: 5 August 2026

J., Bianchi, T. S., Chmura, G. L., Eyre, B. D., Fourqurean, J. W., Hall-Spencer, J. M., Huxham, M., Hendriks, I. E., Krause-Jensen, D., Laffoley, D., Luisetti, T., Marbà, N., Masque, P., McGlathery, K. J., Megonigal, J. P., Murdiyarso, D., Russell, B. D., Santos, R., Serrano, O., Silliman, B. R., Watanabe, K., and Duarte, C. M.: The future of Blue Carbon science, Nat. Commun., 10, 3998-, https://doi.org/10.1038/S41467-019-11693-W, 2019.

Mäkelin, S., Lewandowska, A. M., Rodil, I. F., Karlson, A. M. L., Humborg, C., and Villnäs, A.: Linking Resource Quality and Biodiversity to Benthic Ecosystem Functions Across a Land-to-Sea Gradient, Ecosystems, 27, 329–345, https://doi.org/10.1007/s10021-023-00891-9, 2024.

McLeod, E., Chmura, G. L., Bouillon, S., Salm, R., Björk, M., Duarte, C. M., Lovelock, C. E., Schlesinger, W. H., and Silliman, B. R.: A blueprint for blue carbon: Toward an improved understanding of the role of vegetated coastal habitats in sequestering CO2, Front. Ecol. Environ., 9, 552–560, https://doi.org/10.1890/110004, 2011.

Myllykangas, J. P., Jilbert, T., Jakobs, G., Rehder, G., Werner, J., and Hietanen, S.: Effects of the 2014 major Baltic inflow on methane and nitrous oxide dynamics in the water column of the central Baltic Sea, Earth System Dynamics, 8, 817–826, https://doi.org/10.5194/esd-8-817-2017, 2017.

Niemistö, J. and Lund-Hansen, L. C.: Instantaneous Effects of Sediment Resuspension on Inorganic and Organic Benthic Nutrient Fluxes at a Shallow Water Coastal Site in the Gulf of Finland, Baltic Sea, Estuaries and Coasts, 42, 2054–2071, https://doi.org/10.1007/s12237-019-00648-5, 2019.

Nishant, N., Pykäri, J., Lammerant, R., Villnäs, A., Gustafsson, C., Norkko, A., Cowie, G., and Jilbert, T.: Sedimentary carbon stocks and microbial turnover in shallow coastal areas of the Baltic Sea, Zenodo [data set] https://doi.org/10.5281/zenodo.21512381, 2026.

Pajunen, H.: Carbon in Finnish lake sediments, Hannu Pajunen., Geological Survey of Finland, Espoo, 92 pp., 2000.

Rodil, I. F., Attard, K. M., Norkko, J., Glud, R. N., and Norkko, A.: Estimating Respiration Rates and Secondary Production of Macrobenthic Communities Across Coastal Habitats with Contrasting Structural Biodiversity, Ecosystems 2019 23:3, 23, 630–647, https://doi.org/10.1007/S10021-019-00427-0, 2019.

Rodil, I. F., Attard, K. M., Gustafsson, C., and Norkko, A.: Variable contributions of seafloor communities to ecosystem metabolism across a gradient of habitat-forming species, Mar. Environ. Res., 167, https://doi.org/10.1016/j.marenvres.2021.105321, 2021.

Röhr, M. E., Boström, C., Canal-Vergés, P., and Holmer, M.: Blue carbon stocks in Baltic Sea eelgrass (Zostera marina) meadows, Biogeosciences, 13, 6139–6153, https://doi.org/10.5194/bg-13-6139-2016, 2016.

Röhr, M. E., Holmer, M., Baum, J. K., Björk, M., Chin, D., Chalifour, L., Cimon, S., Cusson, M., Dahl, M., Deyanova, D., Duffy, J. E., Eklöf, J. S., Geyer, J. K., Griffin, J. N., Gullström, M., Hereu, C. M., Hori, M., Hovel, K. A., Hughes, A. R., Jorgensen, P., Kiriakopolos, S., Moksnes, P. O., Nakaoka, M., O'Connor, M. I., Peterson, B., Reiss, K., Reynolds, P. L., Rossi, F., Ruesink, J., Santos, R., Stachowicz, J. J., Tomas, F., Lee, K. S., Unsworth, R. K. F., and Boström, C.: Blue Carbon Storage Capacity of Temperate Eelgrass (Zostera marina) Meadows, Global Biogeochem. Cycles, 32, 1457–1475, https://doi.org/10.1029/2018GB005941, 2018.

https://doi.org/10.5194/egusphere-2026-4456
Preprint. Discussion started: 5 August 2026

Scheffold, M. I. E. and Hense, I.: Quantifying Contemporary Organic Carbon Stocks of the Baltic Sea Ecosystem, Front. Mar. Sci., 7, https://doi.org/10.3389/fmars.2020.571956, 2020.

Schulz, H. D.: Quantification of early diagenesis: Dissolved constituents in pore water and signals in the solid phase, in: Marine Geochemistry, Springer Berlin Heidelberg, 73–124, https://doi.org/10.1007/978-3-662-04242-7_3, 2006.

Smeaton, C. and Austin, W. E. N.: Quality Not Quantity: Prioritizing the Management of Sedimentary Organic Matter Across Continental Shelf Seas, Geophys. Res. Lett., 49, https://doi.org/10.1029/2021GL097481, 2022.

Srithongouthai, S. and Tada, K.: Diffusive Fluxes across Sediment–Water Interface in the Seto Inland Sea, Japan, IARJSET, 2, 71–75, https://doi.org/10.17148/iarjset.2015.21115, 2015.

Sturm, K., Keller-Lehmann, B., Werner, U., Raj Sharma, K., Grinham, A. R., and Yuan, Z.: Sampling considerations and assessment of Exetainer usage for measuring dissolved and gaseous methane and nitrous oxide in aquatic systems, Limnol. Oceanogr. Methods, 13, 375–390, https://doi.org/10.1002/lom3.10031, 2015.

Uth, C., Asmala, E., and Lewandowska, A. M.: Phytoplankton community composition as a driver of annual autochthonous organic carbon dynamics in the northern coastal Baltic Sea, Mar. Ecol. Prog. Ser., 745, 13–24, https://doi.org/10.3354/meps14685, 2024.

Vallius, H.: Permanent seafloor anoxia in coastal basins of the northwestern Gulf of Finland, Baltic Sea, Ambio, 35, 105–108, https://doi.org/10.1579/0044-7447(2006)35[105:psaicb]2.0.co;2, 2006.

Veselić, D. R., Slijepčević, N., Tenodi, S., Pejin, Đ., Jevrosimov, I., Srebro, T. M., and Pilipović, D. T.: From sink to strategy: Sediments at the nexus of carbon sequestration and climate action, Earth. Sci. Rev., 271, https://doi.org/10.1016/j.earscirev.2025.105310, 2025.

Villnäs, A., Norkko, J., Lukkari, K., Hewitt, J., and Norkko, A.: Consequences of Increasing Hypoxic Disturbance on Benthic Communities and Ecosystem Functioning, PLoS One, 7, https://doi.org/10.1371/journal.pone.0044920, 2012.

Villnäs, A., Janas, U., Josefson, A. B., Kendzierska, H., Nygård, H., Norkko, J., and Norkko, A.: Changes in macrofaunal biological traits across estuarine gradients: Implications for the coastal nutrient filter, Mar. Ecol. Prog. Ser., 622, 31–48, https://doi.org/10.3354/meps13008, 2019.

Virta, L., Gammal, J., Järnström, M., Bernard, G., Soininen, J., Norkko, J., and Norkko, A.: The diversity of benthic diatoms affects ecosystem productivity in heterogeneous coastal environments, Ecology, 100, e02765, https://doi.org/https://doi.org/10.1002/ecy.2765, 2019.

Virtanen, E. A., Norkko, A., Nyström Sandman, A., and Viitasalo, M.: Identifying areas prone to coastal hypoxia - The role of topography, Biogeosciences, 16, 3183–3195, https://doi.org/10.5194/bg-16-3183-2019, 2019.

Virtasalo, J. J., Kohonen, T., Vuorinen, I., and Huttula, T.: Sea bottom anoxia in the Archipelago Sea, northern Baltic Sea - Implications for phosphorus remineralization at the sediment surface, Mar. Geol., 224, 103–122, https://doi.org/10.1016/j.margeo.2005.07.010, 2005.

https://doi.org/10.5194/egusphere-2026-4456
Preprint. Discussion started: 5 August 2026

Virtasalo, J. J., Kotilainen, A. T., Räsänen, M. E., and Ojala, A. K.: Late-glacial and post-glacial deposition in a large, low relief, epicontinental basin: The northern Baltic Sea, Sedimentology, 54, 1323–1344, https://doi.org/10.1111/j.1365-3091.2007.00883.x, 2007.

Weiss, R. F. and Price, B. A.: Nitrous oxide solubility in water and seawater, Mar. Chem., 8, 347–359, https://doi.org/10.1016/0304-4203(80)90024-9, 1980.

Wiesenburg, D. A. and Guinasso, N. L. Jr.: Equilibrium solubilities of methane, carbon monoxide, and hydrogen in water and sea water, J. Chem. Eng. Data, 24, 356–360, https://doi.org/10.1021/je60083a006, 1979.

Wikström, S. A., Gubri, B., Asplund, M. E., Dahl, M., Gullström, M., Hansen, J. P., Kumblad, L., Rydin, E., Garbaras, A., and Björk, M.: Influence of landscape characteristics and submerged aquatic vegetation on sediment carbon and nitrogen storage in shallow brackish water habitats, Sci. Rep., 15, https://doi.org/10.1038/s41598-025-92217-z, 2025.

Winterhalter, B.: Late-Quaternary stratigraphy of Baltic Sea basins - a review, Bulletin of the Geological Society of Finland, 64, 189–194, https://doi.org/10.17741/bgsf/64.2.007, 1992.